Practical Thermal Control by Thermo-Electric Actuators

Rob van Gils*[1]

[1] Philips Innovation Services, Eindhoven, the Netherlands

* Corresponding Author: rob.van.gils@philips.com, +31 (0)6 4684 8367

Abstract

In this study a practically feasible Input-Output linearizing feedback law is introduced and tested on an experimental setup. The test setup is representative of part of a medical handheld diagnostics device, requiring fast and accurate temperature control in large temperature ranges. The setup is modelled with an in-house developed lumped mass modelling tool to allow for efficient controller design and synthesis. Furthermore, the setup is controlled via a National Instruments DAQ-unit that communicates with Matlab Simulink on a Windows-based computer. The building blocks in Simulink enabling this are also in-house developed. Experimental results show that the practically feasible control law is capable of dealing with large temperature variations in the setup as well as high frequent fluctuations in the setpoints.

1 Introduction

1.1 Motivation

Consumer electronics, and professional equipment alike, become increasingly reliant upon the ability for precise thermal management. Challenges range from (air-only) high heat flux cooling to precise thermal conditioning of high performance components. As such, thermal control is gaining more attention in the design of these devices.

Moreover, in recent decades a lot of research has been done after new innovations and solutions for health, including the development of new (automated) diagnostics platforms for the world's common diseases [1]. Handheld devices are designed to-be-used for the handling and diagnostics of extremely small fluid volumes (e.g. blood, saliva) to significantly reduce analysis time and reagent costs [2]. Important facets for the success of these devices are small size and ability for accurate temperature control.

Furthermore, the replacement of light sources in many fields (such as indoor, outdoor and automotive lighting, screen backlighting and guideboards) by LED lighting is continuing. The nature of LEDs is such that an increase in temperature leads to reduction in light output and quality and LED lifetime. For this reason, the heat generated by LEDs should be *controlled* (especially for high power LEDs) via an efficient cooling system and extracted from the LED device [3].

Peltier elements or in short 'peltiers' are thermo-electric coolers (TECs) that can be used either for heating or for cooling (in practice their main application is cooling). Its main advantages compared to e.g. a vapour-compression refrigerator are its lack of moving parts or circulating liquid, (long life in quasi static conditions), invulnerability to potential leaks, and its *small size* and *flexible shape*. Therefore, they are ideal as thermal actuators in the electronics described above. Moreover, since they allow for higher heat sink temperatures (and thus for smaller heat sink volumes) without compromising component temperatures, their application can meet tight volume constraints. The main disadvantages of peltiers are high cost, poor power efficiency, sensitivity for mechanical stresses and low electrical impedance.

1.2 Background

TECs operate by the Peltier effect (which also goes by the more general name thermoelectric effect). The device has two sides, connected by thermoelectric legs or pellets, pairs of N- and P-type semiconductors, which are placed thermally in parallel and electrically in series, see Figure 1. When DC current flows through the device, it brings heat from one side to the other, so that one side gets cooler while the other gets hotter, generating a "hot" and a "cold" side. The hot side is attached to a heat sink so that it remains close to ambient temperature, while the cold side goes below room temperature, see e.g. [4].

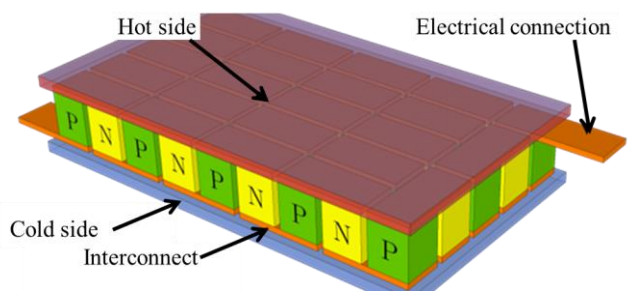

Figure 1: Peltier (or Thermo-Electric Cooler) schematic

Thermal control/actuation by peltier devices has been investigated in a wide variety of studies [5]. For example in [6, 7] the device was used to construct a virtual thermal resistance. But most investigations focus on effective control of the peltier cold-side, see e.g. [8, 9, 10, 11]. Mathematical models describing the thermal behaviour of peltier elements can be found in among others [4, 5, 9].

Although various control strategies have been studied, the linear proportional-integral-differential (PID) controllers or switching PID controllers are commonly used for their simplicity in both design and implementation [8]. However,

due to their nonlinear behaviour, controlling the cold side temperature of peltiers is not simple. Linear PID control might work in some cases but is not robust, see [9]. On the other side, other studies that consider nonlinear controller techniques do not consider practical limitations in their controller design. Therefore in this study a generic Input-Output (IO) linearizing feedback law for Peltier devices is investigated, while explicitly modelling the effects that degrade the control performance when going from theoretical model to practical setup. This results in increased performance and larger robustness regimes, see also [12].

1.3 Outline

In Section 2 the methodology for investigation of the practical control schemes is discussed. The experimental setup and the corresponding thermal model are clarified. In Section 3 the IO linearizing feedback law is introduced, while keeping focus on practical implementation. In Section 4 the practically feasible control law is put to the test in several experiments. Finally in Section 5 conclusions are drawn and an outlook on future work is given.

2 Methodology

2.1 Experimental Setup

In this study the practical effectiveness of the IO linearizing feedback law is investigated by means of a simple test setup representative of part of a handheld diagnostic device. The setup is depicted in Figure 2. It consists of a stainless steel bottom plate that is divided in two sections that must be thermally controlled individually. To this end two peltiers are placed between the bottom plate and the aluminum top plate. The latter is connected to a fanned heat sink.

The setup is controlled using the thermal control platform: a Windows-based computer running Matlab Simulink with in-house developed software to communicate with a USB-based National Instruments DAQ-unit for the importing and exporting of signals, see Figure 3. The Matlab Simulink environment allows for quick and flexible controller design for every setup. Moreover, it allows for the use of standard control theory due to the extensive Systems Control toolbox.

2.2 Thermo-dynamical Model

In order to calculate appropriate controller settings the experimental setup is modeled using the Philips Advanced Lumped Mass (PALM)-tool. This is a set of in-house developed Matlab macros that allow for the efficient design of advanced (thermal) lumped mass models. A schematic overview of the model of the setup is given in Figure 4. The top and bottom plate are divided in four masses each: two directly adjacent to the peltiers and one mass to represent the plate around each TEC. More masses are not needed as the characteristic length of the bottom plate equals 7.5cm, while its dimensions are only 10x10 cm^2, see [13]. The heat sink (HS) is divided in a left and right side and base and fins.

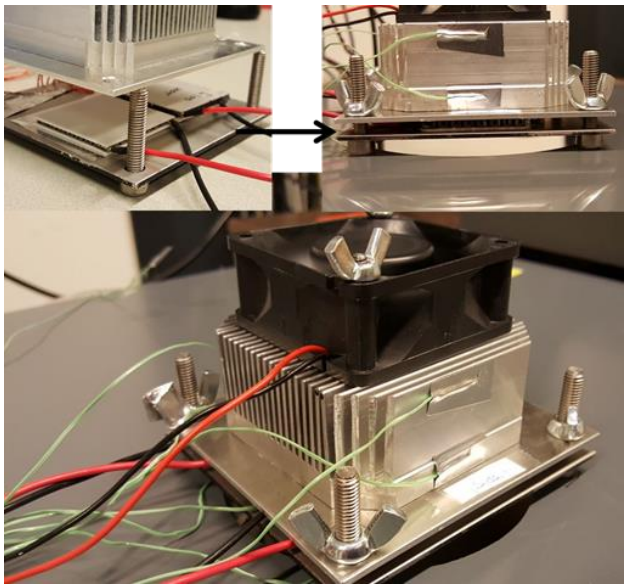

Figure 2: Experimental setup

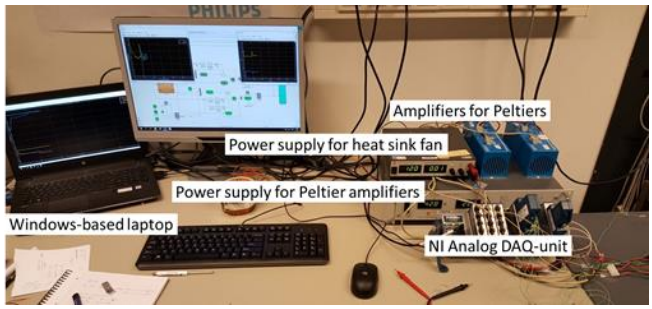

Figure 3: Data Acquisition setup

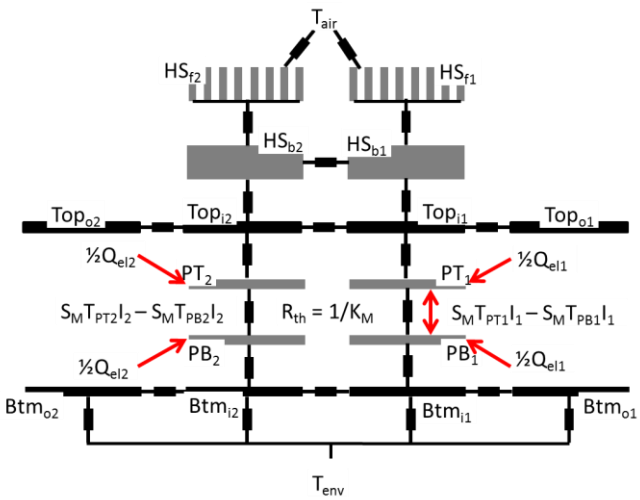

Figure 4: Schematic of the lumped mass model

In this model most masses can be connected straightforwardly via linear thermal resistances. Therefore the modeling details for these parts are omitted here and only the mathematical relations describing the peltier thermal behavior are discussed.

The governing equations for the peltier behaviour can be found using the physical relations describing the thermo-electric behavior. If DC current runs through the peltier device, heat is extracted from the cold side by the 'Peltier effect'. The amount of heat is quantified by the device's Seebeck coefficient, S_M, the DC current, I, and the temperature of the cold side, T_c, via

$$Q_{peltier,c} = S_M T_c I. \quad (1)$$

Analogously the heat *dumped* at the hot side equals:

$$Q_{peltier,h} = S_M T_h I. \quad (2)$$

Besides the heat pumped from cold to hot side, also heat is generated in the thermoelectric pairs due to electrical losses. It is assumed (this is commonly done in peltier analysis) that half of this heat will flow to the hot side and half will flow to the cold side. The heat generated, Q_{el}, is quantified by the DC current and the device resistivity R_M via

$$Q_{el} = R_M I^2. \quad (3)$$

Finally heat is transported from hot to cold side due to thermal conduction caused by the temperature gradient over the legs. This leakage is quantified by the device thermal conductivity K_M and equals

$$Q_{leak} = K_M(T_h - T_c). \quad (4)$$

The differential equations defining the hot and cold side temperature then readily follow from these heat flows, this yields a nonlinear and non-affine peltier model

$$m_h c_{p,h} \dot{T_h} = S_M T_h I + \tfrac{1}{2} R_M I^2 - K_M(T_h - T_c), \quad (5)$$

$$m_c c_{p,c} \dot{T_c} = -S_M T_c I + \tfrac{1}{2} R_M I^2 + K_M(T_h - T_c), \quad (6)$$

where T_h and T_c are the hot and cold plate temperature respectively. Biot and Fourier number analyses show that this approach is valid in the parameter space of interest. Moreover, numerical analyses indicate that not modelling the thermoelectric legs introduces only a small error.

The total model of the setup can be written as:

$$E\dot{x} = Ax + Bu + F_{nl}, \quad (7)$$

where the state-vector x is of size 16x1, and contains the temperatures of the 16 lumped masses, and the input vector u is of size 2x1 and contains the external temperatures T_{env} and T_{air}. Furthermore, the matrix E contains the capacities of the masses, A is the system matrix and B the input matrix. Finally, the nonlinear vector function F_{nl} equals

$$F_{nl} = \begin{bmatrix} S_M x_1 I_1 + \frac{1}{2} R_M I_1^2 - K_M(x_1 - x_2) \\ -S_M x_2 I_1 + \frac{1}{2} R_M I_1^2 + K_M(x_1 - x_2) \\ S_M x_3 I_2 + \frac{1}{2} R_M I_2^2 - K_M(x_3 - x_4) \\ -S_M x_4 I_2 + \frac{1}{2} R_M I_2^2 + K_M(x_3 - x_4) \\ \mathbf{0} \end{bmatrix}. \quad (8)$$

Note that x_1 and x_3 are the peltier tops and x_2 and x_4 the peltier bottoms of peltier 1 and 2, respectively.

2.3 Setup Identification & Model Validation

The parameters for the peltiers considered are determined using the thermal control platform. The device conductivity K_M can be easily determined by applying a heat load (e.g. with a foil heater) to the bottom plate and determining its temperature rise relative to that of the top plate. S_M and R_M can then be determined by increasing the peltier current until the bottom and top plate are at equal temperature. If top and bottom plate are at equal temperature, R_M readily follows via $R_M = V/I$. S_M in turn follows from the heat that must be transferred to the top (i.e. heater power, Q, and half of the electrical losses $\frac{1}{2}R_M I^2$) via $S_M = (Q+\frac{1}{2}R_M I^2)/(T_c I)$. Note that this can be done at different temperatures to also find temperature dependencies. The average parameters of the peltiers used, in this way have been determined to be S_M = 0.0509V/K, R_M = 3.34Ω and K_M = 0.394W/K.

The setup contains two peltiers, that can be actuated individually (note that it is assumed the peltiers are governed by the same parameters). To validate the model, both peltiers are subjected to different input currents and both the resulting peltier voltage as well as the cold side temperatures are logged and compared to simulations. The results are shown in Figure 5. Clearly the simulated values correspond very well with the measured values. Moreover, the simulated and measured resulting peltier voltages also overlap (not shown in figure), establishing the validity of the model. Hence, the model can be used to investigate different controller techniques and synthesize controller parameters.

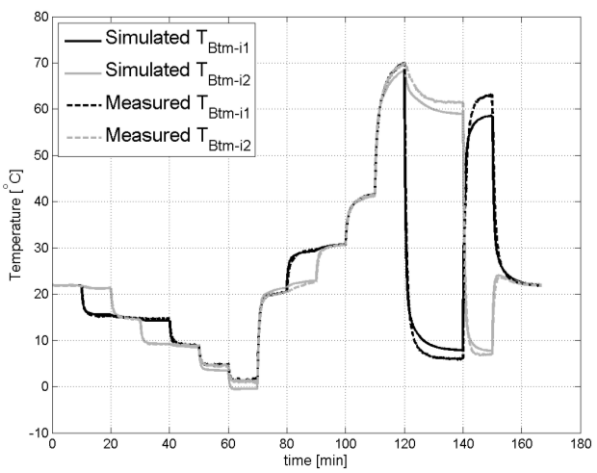

Figure 5: Temperatures: measurement vs simulation

3 Input/Output Linearization

Linear control via feedback of the cold side temperature can be done in some cases for peltiers. Implementation and design of such controllers is straightforward. However, due to the nonlinear nature of the peltier dynamics, the linear control theory is valid only in a very narrow operating range. Unstable behavior of a previously stable plant can occur rapidly if the heat load at the peltier bottom is shortly increased or if a different temperature setpoint is required.

3.1 Input-Output Linearization in Theory

An IO linearizing feedback is a control strategy in which the input current is chosen such that the relation between a new input u and the output (in this case the bottom of peltier 1, denoted by T_{PB1}) is linear. The main advantage of this strategy is that a linear controller can be designed that is stable in the entire operating range and exhibits the same behavior (i.e. with respect to settling time, overshoot etc.) for different setpoints.

Prescribing the input current to the i-th peltier as

$$I_i = \frac{S_M T_{PBi}}{R_M} - \sqrt{\frac{S_M^2 T_{PBi}^2}{R_M^2} + \frac{u_i}{1/2 R_M}}, \tag{9}$$

and substituting it in (8) leaves

$$F_{nl,2} = u_1 + K_M(x_1 - x_2), \tag{10}$$

for the second element of the vector F_{nl}. Note that this linearizes the entire differential equation (DE) that governs the peltier bottom temperature. By taking u_1 as

$$u_1 = -\frac{1}{\tau_{c1}}(T_{PB1} - T_{set1}) - K_M(x_1 - x_2) - A_{2,:}x, \tag{11}$$

the DE for the peltier bottom temperature reduces to a 1st order linear response with time constant τ_{c1}. Here $A_{2,:}$ means only the second row of the matrix A is considered. The same approach can be followed to linearize the input-output behavior for the second peltier.

3.2 Input-Output Linearization in Practice

As discussed in Section 3.1, ideally the peltier bottom temperatures can be set to follow a reference with a given time constant. However, in practice a few limitations arise. Firstly the input u_i in (9) must satisfy

$$u_i \geq -\frac{S_M^2 T_{PBi}^2}{2R_M}, \tag{12}$$

in order for the square root term in (9) to be ≥ 0. With this square root term equal to 0, the input current reduces to $I = S_M T_{PBi}/R_M$, which equals the optimal current for which the net heat extraction from the cold side is maximal. Higher currents would lead to more heat dissipation and thus a smaller net heat extraction. This effect is known to cause thermal runaway in PID controlled peltier setups.

Secondly in practice not all lumped mass temperatures can be measured, while they are required in (11) to reduce the DE to a 1st order linear system. Moreover, the controlled temperature, T_{PBi}, often is not accessible. In our case it must be replaced with the bottom plate temperature, T_{Btmi}, instead.

Thirdly, the modeling might not be ideal and all effort in reducing the DEs for the peltier bottoms to a 1st order linear system are in vain. Therefore, the input u_i can better be replaced with a PI-control scheme:

$$\begin{aligned} \dot{e}_I &= T_{Btmi} - T_{seti}, \\ u_i &= -\frac{1}{\tau_{ci}}(T_{Btmi} - T_{seti}) - K_I e_I - K_M(T_{HSbi} - T_{Btmi}). \end{aligned} \tag{13}$$

Note that the limitation on the input u_i, see (12), remains. In (13), e_I is the integral of the tracking error, thus generating an I-action in the control law u_i, see e.g. [14]. Especially, the need for an I-action introduces standard linear control issues like the need to find a compromise between settling time and overshoot.

4 Experimental Results

The practically feasible control law (13) is implemented in the Simulink scheme that drives the peltier devices. To show its effectiveness, the peltiers are set to follow three different reference signal combinations.

4.1 Sinusoidal Reference Tracking

In the first combination the cold-side of the first peltier is to follow a sinusoidal with an amplitude of 4K, a mean at 18°C and a period time of 300 seconds, while the second TEC must follow a sinusoidal with an amplitude of 10K, a mean at 22°C and a period time of 400 seconds. That is the reference signals are given by

$$\begin{aligned} R_1(t) &= 18 + 4\sin(2\pi/300 \cdot t), \\ R_2(t) &= 22 + 10\sin(2\pi/400 \cdot t). \end{aligned} \tag{14}$$

The results of the experiment are depicted in Figure 6. As can be seen, both peltiers follow their reference without being influenced by the setpoint of the other peltier. The tracking error is in the order of 5%. Note that the tracking error is highly variant under the amplitude and frequency of the sinusoid and that relatively much thermal mass must be cycled in this experiment due to the stainless steel bottom plate under the peltiers.

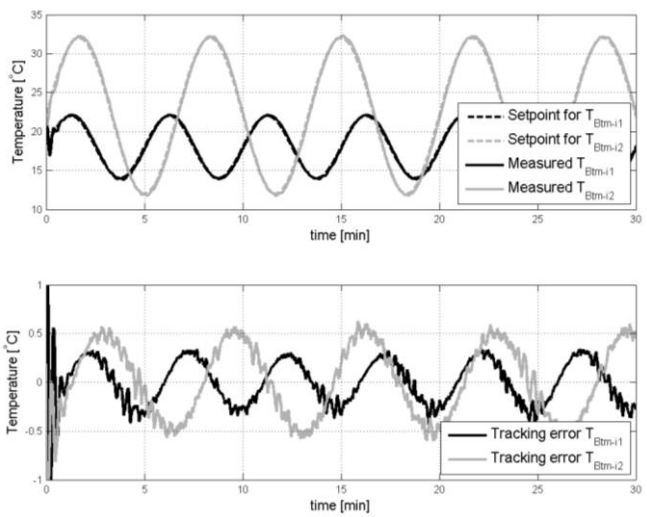

Figure 6: Bottom plate temperatures with references following (14). Top figure: temperatures, bottom figure: tracking errors.

4.2 Pulsed Reference Tracking

In the second reference combination, the peltiers are forced to follow pulses. The reference signals are defined by

$$R_1(t) = 30 + 10 \cdot \text{sign}(\sin(2\pi/600 \cdot t)),$$
$$R_2(t) = 20 + 5 \cdot \text{sign}(\sin(2\pi/400 \cdot t)). \quad (15)$$

In linear control it is commonly known that with PI-control always a compromise between settling time and overshoot must be made. Therefore in this experiment the first peltier is set to reach its setpoint as fast as possible, accepting the corresponding overshoot, while the second peltier is set to decently converge to the setpoint via a 1st order linear response with a time constant of 20 seconds.

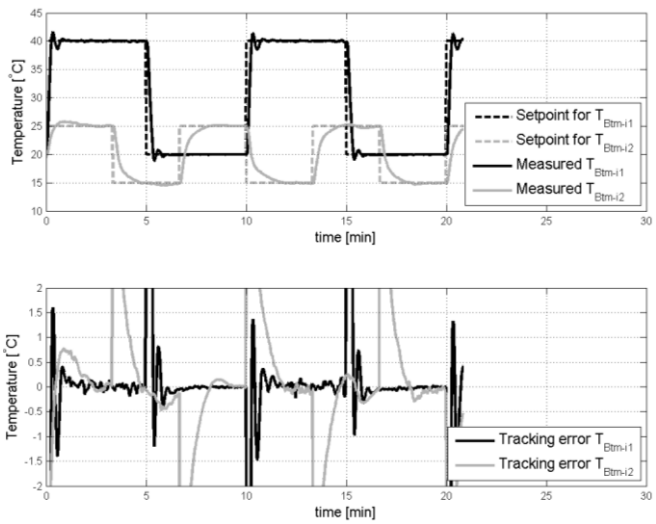

Figure 7: Bottom plate temperatures with references following (15). Top figure: temperatures, bottom figure: tracking errors.

The results of this experiment are shown in Figure 7. As can be seen the first peltier tries to reach its setpoint as fast as possible after a step in the reference. This results in overshoot (~6%) of the setpoint, which is acceptable. The second peltier converges to its setpoint with a first order response with τ = 20sec. To emphasize this, in Figure 8, the response is plotted from 200 to 600 seconds together with the 1st order response.

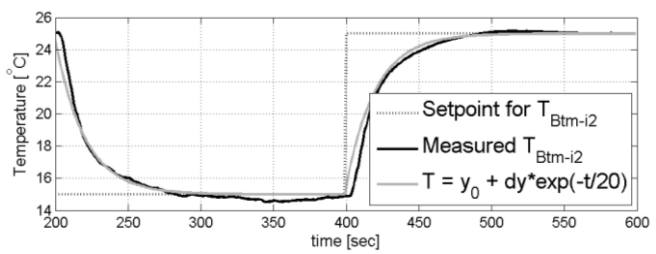

Figure 8: Response of peltier 2 together with a 1st order response with τ = 20sec.

4.3 Pulsed Reference Tracking with Large dT

Finally, the IO linearizing feedback is put to the test by forcing the first peltier to follow a pulsed function with large amplitude while the second peltier is to maintain a constant temperature. References are defined following

$$R_1(t) = 45 + 30 \cdot \text{sign}(\sin(2\pi/1200 \cdot t))$$
$$R_2(t) = 10 \quad (16)$$

The results of this experiment are shown in Figure 9. As can be seen the control law even manages to overcome the 60K temperature step without any abnormalities. Again the setpoint is reached as fast as possible considering peltier limitations. This time it introduces an overshoot of 7K (≈11%), meaning the linear character of the control law is not maintained completely (overshoots should scale linearly), this is the result of modeling inaccuracies and parameter nonlinearities. Nonetheless the control law is fit to stabilize the input output behavior.

The bottom of the second peltier must be kept at 10°C even during the interference of the evolution of the first peltier. As can be seen, the control law succeeds in this with a tracking error of only 0.4K. It is noteworthy to mention that the tracking error is considerably lower in the timeframe that the first peltier is at 15°C, showing the influence of the first peltier on the second peltier tracking error.

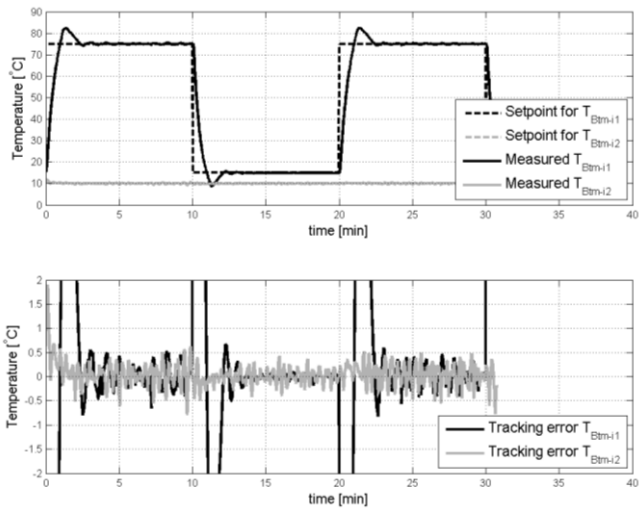

Figure 9: Bottom plate temperatures with references following (16). Top figure: temperatures, bottom figure: tracking errors.

For the sake of completeness in Figure 10 an IR-picture of the bottom plate temperature is shown (note that the bottom is coated for IR-compatibility). The picture is taken at t = 9min of the experiment shown in Figure 9. Note that the temperature sensor of peltier 2 is not placed in the exact cold spot of the plate, next to the sensor a region with T = 6-8°C exist. The bottom plate temperature of the first TEC is uniform at ~75°C.

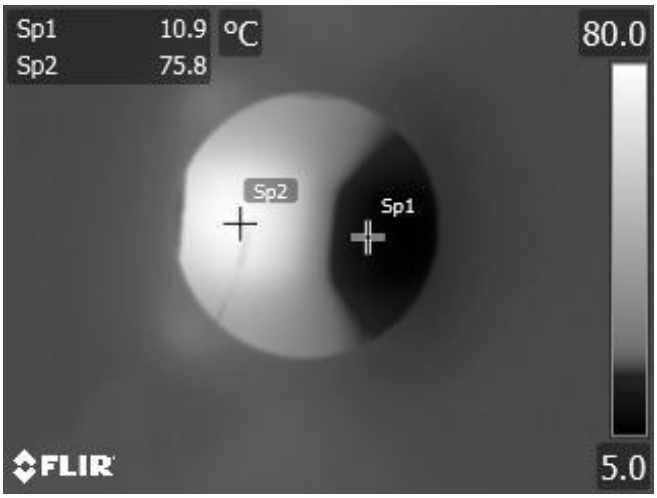

Figure 10: IR picture of bottom plate, with T_{set1} = 75°C and T_{set2} = 10°C.

5 Conclusions & Future Work

5.1 Conclusions

In this study a practically feasible IO linearization scheme is tested on an experimental setup representative of a part of a handheld diagnostic device. The added value compared to other studies can be found in the explicit modeling of effects that degrade the control performance when going from an ideal model to a practical test setup.

To that purpose, a standard IO linearizing feedback is extended with a PI-control law to perform fast and accurate temperature control on two individual peltier devices that influence each other via thermal connection through a stainless steel bottom plate.

Experimental results show that the adapted IO linearizing feedback law is very suitable for control of peltier elements in practical applications. Both sinusoidal references as well as pulsed step references can be followed adequately. Nevertheless, the well-known compromise between settling time and overshoot must be considered in the PI-control law of the IO linearizing feedback. The PI-control law seems stable in the entire application range though.

5.2 Future Work

In order to further improve the closed-loop performance of this test setup the practically feasible control law should be designed to more closely mimic the ideal IO-linearization case. To that end a non-linear observer could be implemented in order to estimate the temperature states that cannot be measured. This potentially could eliminate the overshoot during pulsed references. This will be investigated in the future.

Acknowledgements

This study has been performed using the Philips Innovation Services Thermal Control Platform. This platform consists of in-house developed software to be able to real-time use Matlab Simulink for data acquisition and manipulation of thermal systems. Andre Faesen and Joost Groenen are highly acknowledged for the creation of this software.

Literature

[1] P. Yager, T. Edwards, E. Fu, K. Helton, K. Nelson, M. Tam and B. Weigl, “Microfluidic diagnostic technologies for global public health” Nature vol.442, pp. 412-418, 2006.

[2] J. Jiang, G. Kaigala, H. Marquez and C. Backhouse, “Nonlinear controller designs for thermal management in pcr amplification”, IEEE Transactions on Control Systems Technology, vol. 20, pp. 11-30, 2012.

[3] M. Kaya, “Experimental study on active cooling systems used for thermal management of high-power multichip light-emitting diodes”, The Scientific World Journal, vol. 2014.

[4] A. Pettes, M. Hodes and K. Goodson, “Optimized thermoelectric refrigeration in the presence of thermal boundary resistance” IEEE Transactions on advanced packaging, vol. 32, pp. 423-430, 2009.

[5] C. Zhang, J. Xu, W. Ma and W. Zheng “PCR microfluidic devices for DNA amplification” Biotechnology advances, vol. 24, pp.243–284, 2006.

[6] V. Székely, A. Nagy, S Torok, G. Hajas and M Rencz, “Realization of an electronically controlled thermal resistance”, Microelectronics Journal, vol.31, pp. 811-814, 2000.

[7] V. Székely, S. Torok, E. Kollar, “Improvements of the variable thermal resistance”, 13th Therminic International workshop, 2007.

[8] J. Khandurina, T. McKnight, S. Jacobsen, L. Waters, R. Foote and J. Ramsey, “Integrated system for rapid PCR-based DNA analysis in microfluidic devices”, Analytical Chemistry, vol. 72, pp. 2995–3000, 2000.

[9] J. Jiang, “Nonlinear controller designs for thermal management in PCR amplification”, IEEE Transactions on Control Systems Technology, vol. 20, pp. 11-30, 2012.

[10] R. Zhang, D. Brooks, M. Hodes and V. Manno, “Optimized thermoelectric module-heat sink assemblies for precision temperature control”, Journal of Electronic Packaging, vol. 134, 2012.

[11] Juan Chen, Thermal controller design for a lab-on-chip benchmark, Master’s Thesis, Eindhoven University of Technology, 2013

[12] H. Khalil, “Nonlinear systems”, Prentice Hall, 3rd edition, 2002.

[13] W. Luiten, “Characteristic length and cooling circle”, 26th Annual IEEE Semiconductor Thermal Measurement and Management Symposium, 2010

[14] T. Kailath, “Linear systems”, Prentice Hall, 1st edition, 1980.